Three-Dimensional Self-Similarity of Coalescing Viscous Drops in the Thin-Film Regime

Paul R. Kaneelil,[1] Amir A. Pahlavan,[2] Nan Xue,[1,3] and Howard A. Stone[1,*]
[1]Department of Mechanical and Aerospace Engineering, Princeton University, Princeton, New Jersey 08544, USA
[2]Department of Mechanical Engineering and Material Science, Yale University, New Haven, Connecticut 06511, USA
[3]Department of Materials, ETH Zürich, 8093 Zürich, Switzerland

(Received 18 May 2022; accepted 8 September 2022; published 28 September 2022)

Coalescence and breakup of drops are classic problems in fluid physics that often involve self-similarity and singularity formation. While the coalescence of suspended drops is axisymmetric, the coalescence of drops on a substrate is inherently three-dimensional. Yet, studies so far have only considered this problem in two dimensions. In this Letter, we use interferometry to reveal the three-dimensional shape of the interface as two drops coalescence on a substrate. We unify the known scaling laws in this problem within the thin-film approximation and find a three-dimensional self-similarity that enables us to describe the anisotropic shape of the dynamic interface with a universal curve.

DOI: 10.1103/PhysRevLett.129.144501

Whether it is the merging of raindrops on a windshield or morning dew drops on leaves, coalescence is a common phenomenon that occurs all around us and has been the subject of numerous scientific studies [1–4]. On a wetting substrate, two drops of the same liquid placed near one another can spread, make contact, and coalesce, which consists of rearrangement of fluid and topological changes of the fluid-air interface. Some of the previous investigations on coalescence of sessile drops have explored the effects of substrate wettability [5–7], droplet geometry [8,9], asymmetry of shape [10] and of surface tension [11–14] and the influence of surfactants [15].

Unlike the axisymmetric case of coalescence of suspended drops [16,17], the coalescence of sessile drops is fundamentally a three-dimensional (3D) phenomenon, i.e., anisotropic, where the symmetry is broken by the presence of the substrate and the resulting contact line. Thus, the shape of the meniscus bridge that connects the two sessile drops involves two dynamic length scales: the half-width of the meniscus bridge, which scales as $r_m \propto t^{1/2}$ [5], and the height of the bridge, which scales as $h \propto t$ in the lubrication regime [10], $h \propto t^{2/3}$ for intermediate contact angles in the inertial regime, and $h \propto t^{1/2}$ when the contact angle of the drop is 90° in the inertial regime [8]. Despite the three-dimensional nature of the coalescence of sessile drops, all of the studies so far have only considered this problem in two dimensions (2D).

In this Letter, we explore the 3D shape of the interface using interferometry as two viscous drops coalesce on a wetting substrate (Fig. 1). We find that the shape of the interface in the direction of the growing meniscus bridge can be understood geometrically and that the 3D shape of the interface at early times near the coalescence point has a self-similar structure that can be mapped onto a universal curve. We propose a similarity ansatz as a function of one similarity variable to capture the 3D profile. The numerical solution of the self-similar profile is in good agreement with the experimental results. Our results unify the known scaling laws in the viscous regime and provide experimental evidence that supports the assumptions that are commonly made in this problem.

In experiments, two silicone oil drops (density $\rho = 960\ \mathrm{kg/m^3}$) were placed next to each other on a glass microscope slide [Fig. 1(a)]. We explored eight different combinations varying the viscosity $\mu = [51.5, 102, 540]\ \mathrm{mPa\,s}$ and the volume of the drop $V = [0.22 \pm 0.07, 0.45 \pm 0.04, 2.5 \pm 0.2, 6.3 \pm 0.3, 11.7 \pm 0.3]\ \mu\mathrm{l}$. Each experiment was repeated two or three times. The interfacial tensions with air of the three different silicone oils with the given viscosity values were $\gamma = [22.7 \pm 5.4, 20.9 \pm 1.3, 21.1 \pm 1.7]\ \mathrm{mN/m}$, respectively. In all of the experiments performed, the height and the base radius of the drops just before coalescence was approximately $H_0 = \mathcal{O}(0.1)$ mm and $R_0 = \mathcal{O}(1)$ mm, respectively, corresponding to Bond numbers of about $\mathrm{Bo} = \rho g R_0 H_0/\gamma = \mathcal{O}(10^{-2})$, suggesting that gravitational effects can be neglected.

The microscope slides used for the experiments were cleaned by sequentially immersing and sonicating them for 15 min each in a surfactant solution, deionized water, ethanol, and acetone bath. The static advancing contact angle θ of the drops with the substrate at the moment of coalescence, hereafter referred to as the effective contact angle, was within 2° to 4° (0.035 to 0.07 rad), allowing the imaging of the coalescence event using interferometry. The drops are dispensed successively through a needle and are placed far enough apart to spread and reach the small angles before contact. The angles of the drops are measured *a posteriori* from the interferometry images to confirm symmetric coalescence. Our setup consisted of a camera and a helium-neon laser of wavelength $\lambda = 633$ nm that

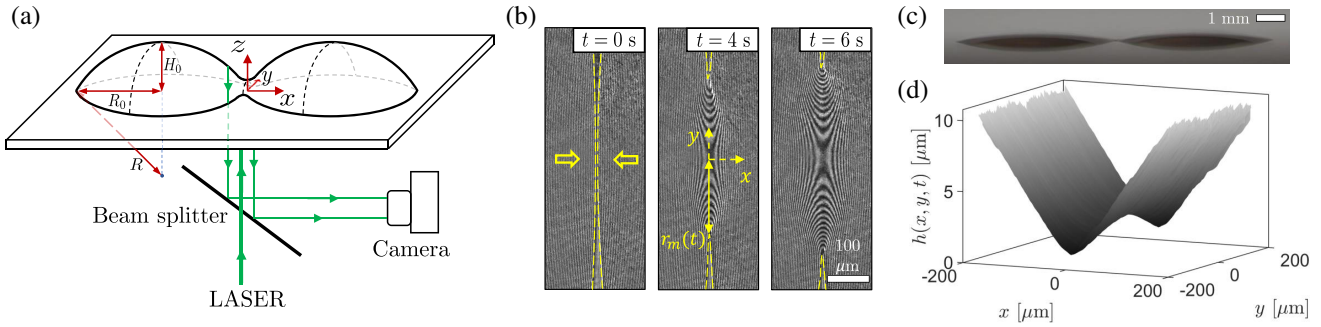

FIG. 1. Three-dimensional reconstruction of the shape of the interface using interferometry. (a) Schematic showing the drop geometry and the interferometry setup used in the experiments. The base radius R_0, height H_0, and the radius of the spherical cap R that describes the shape of the drop at the time of coalescence are labeled. (b) Interferometry images showing two silicone oil drops ($\mu = 102$ mPa s, $V = 2.53$ μl) at $t \approx 0$, 4, and 6 s after coalescence. Dashed yellow lines are guides for the eyes and show the macroscopic contact line of the drops. The half-width of the meniscus bridge is labeled $r_m(t)$. Scale bar represents 100 μm. (c) Side view image of the drops near the time of contact. Scale bar represents 1 mm. (d) Reconstructed 3D shape of the interface at $t \approx 5$ s.

illuminated the interface near the coalescence point, as schematically shown in Fig. 1(a). The interference pattern created by the reflected light from the air-liquid interface and the air-substrate interface was used to measure the height profile. Typical interferometry images during coalescence are shown in Fig. 1(b) and a side view of the drops are shown in Fig. 1(c). The reconstructed shape plotted in Fig. 1(d) shows the anisotropic 3D shape of the interface during coalescence and resembles the shape of a saddle. Here, the part of the saddle that is curved upward is formed by the sides of the two merging drops and the part that is curved downward is the meniscus bridge, which slopes down to a height of zero at the outward-moving contact line. The origin of the axes and the time $t = 0$ correspond to the location and the time when the drops first make contact.

As the drops make contact, a meniscus bridge forms and spreads outward on the substrate in the y direction. The half-width $r_m(t)$ of the meniscus bridge [see Fig. 1(b)] on a completely wetting substrate follows the scaling $r_m(t) \approx H_0^{3/2}/R_0(\gamma t/\mu)^{1/2}$ at early times. Most of the fluid flow driving the growth of this bridge is in the x direction [5]. This one-dimensional (1D) flow assumption holds at early times when the width of the meniscus bridge is much smaller than the contact radii of the spreading drops. Thus, the major component of the fluid velocity field in the drops will be in the x direction locally near the coalescence point.

The 1D flow assumption was used to show the self-similarity of the interface profile along the $y = 0$ plane [10]; see Fig. 2(a) for a schematic. The shape of the interface along this symmetry plane was found to be governed by the height at the initial coalescence point, $h_0(t) = vt$, which scales linearly with time. Assuming that the effective contact angle θ of the drops during coalescence is small, the vertical velocity of the interface can be identified as $v = A(\gamma/3\mu)\theta^4$ from the thin-film equation. Here, A is a numerical prefactor. Rescaling both $h(x, y = 0, t)$ and x with $h_0(t)$ in the 2D thin-film equation, a similarity solution in terms of the variable $\xi = \theta x/h_0(t)$, with no fitting parameters, can be obtained that describes the shape of the interface locally near the coalescence point at early times [10].

Our 3D reconstruction of the meniscus allows us to test whether the self-similarity along the $y = 0$ plane also holds

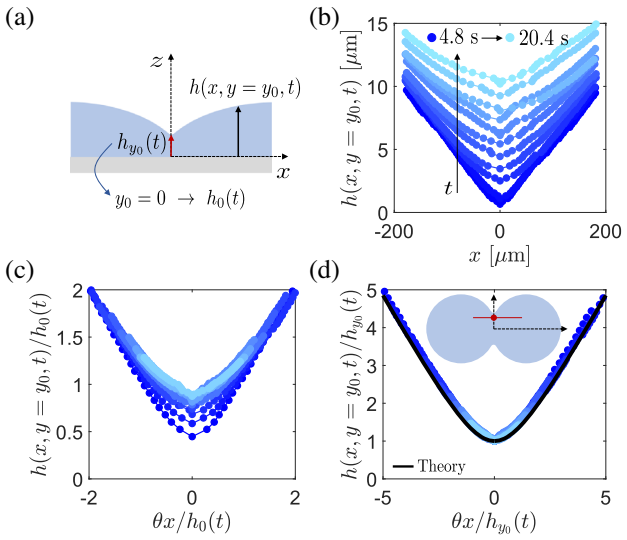

FIG. 2. The height profile in the xz plane at any arbitrary y location is self-similar. (a) Schematic of the height profile along this plane at $y = y_0$, where $h_{y_0}(t)$ is the height at the coalescence point in that plane. (b) Data from an experiment using silicone oil drops with $\mu = 102$ mPa s and $V = 2.53$ μl showing the time evolution of the height profile along the xz plane with $y_0 = 168$ μm. The lines connecting the markers are just guides for the eyes. (c) The height profile rescaled with the height at the initial coalescence point $h_0(t) = vt$. (d) The height profile rescaled with the height at the coalescence point in this specific plane, $h_{y_0}(t)$, shows agreement with the similarity solution (black line [10]). The red dot in the inset is a schematic representation of the location of h_{y_0}.

for $y \neq 0$. Note that the relevant length scale for any off-center plane would be the height at the coalescence point in that specific plane: $h_{y_0}(t) \equiv h(x = 0, y = y_0, t)$. Figure 2(b) shows the temporal evolution of the height profile along an xz plane at $y_0 = 168$ μm. Rescaling the height profile of this off-center plane with the height at the initial coalescence point $h_0(t)$ does not collapse the data [see Fig. 2(c)], whereas rescaling with $h_{y_0}(t)$ does collapse the data and shows agreement with the similarity solution (black line), as shown in Fig. 2(d). This collapse indicates that the underlying 1D flow assumption holds even for $y \neq 0$.

Thus, we have a glimpse of two important attributes of the problem that will be amplified in the rest of this Letter. First, the evolution of the 3D interface is more generally governed by the height along the meniscus bridge $h(x = 0, y, t)$ rather than simply the height at the initial coalescence point $h_0(t)$. Second, as a direct consequence of the first, the scaling parameter for the similarity solution that describes the 3D shape of the interface must have a y dependence, implying a 3D self-similarity. We now reveal the height profile along the liquid meniscus bridge and provide a more general similarity ansatz that can predict the dynamic shape of the anisotropic interface.

Along the yz plane, the coalescence point $h_0(t)$ is the highest point on the interface and the height of the interface vanishes as we approach the edge of the meniscus bridge [see Fig. 3(a)]. Interferometry data showing the evolution of the interface in the yz plane are presented in Fig. 3(b). Given that the flow is mainly in the x direction, we expect the interface profile in the y direction to be set by surface tension forces rather than viscous forces. The geometric shape that minimizes surface energy and is often invoked for studying sessile drops is a spherical cap [18]. We find that the interface profile along the yz plane is a circular segment, a cross section of the spherical cap, and can be modeled as $h(x = 0, y, t) = (a^2 - y^2)^{1/2} - [a - h_0(t)]$, where a is the radius of a circle, as shown in Fig. 3(a). Approximating the equation for the circular segment for $y/a \ll 1$ and rearranging gives

$$\frac{h(x = 0, y, t)}{h_0(t)} = 1 - \frac{1}{2}\left[\frac{y}{\sqrt{a h_0(t)}}\right]^2, \qquad (1)$$

which shows the natural way to rescale the variables and is plotted along with the rescaled experimental data in Fig. 3(c). All of the data that we could resolve with interferometry seem to agree with the predicted geometric shape of the interface although we would expect the height profile to deviate at the molecular scales owing to the presence of a precursor film [19–21].

The dynamic shape of the interface in the yz plane is part of a circle of constant radius a. For the viscously dominated motion resulting from coalescence, we can expect the length scale a to be at most a function of the effective

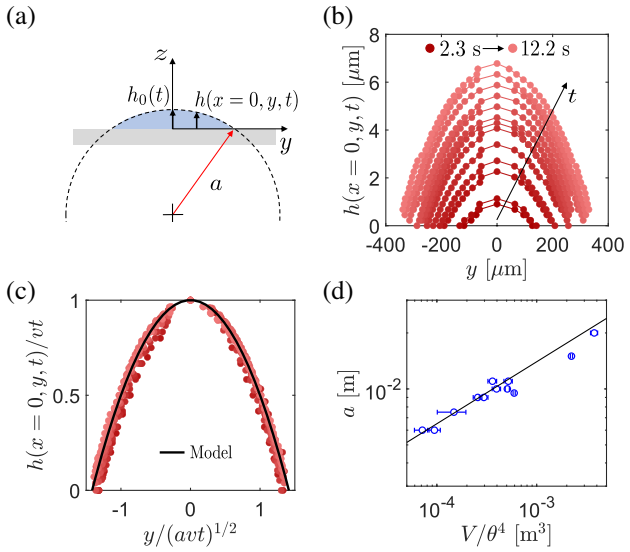

FIG. 3. The height profile along the meniscus bridge in the yz plane is a self-similar parabola. (a) Schematic of the height profile, which resembles a circular segment of radius a. (b) Data from an experiment using silicone oil drops with $\mu = 102$ mPa s and $V = 2.53$ μl showing the time evolution of the height profile. The lines connecting the markers are just guides for the eyes. (c) Rescaled height profile collapses the data and agrees with the proposed model [Eq. (1)]. (d) The value of the length scale a used to collapse all of the experimental data plotted against V/θ^4 follows a $1/3$ power law (black line). The fitted slope was 0.29.

contact angle at the time of coalescence and the volume of the drop: $a = f(\theta)V^{1/3}$. If we assume the shape of the interface in the yz plane as the intersection between two overlapping (static) spherical cap-shaped drops, then a is approximately the radius R of the spherical cap in the limit $\theta \ll 1$ (see Supplemental Material [22], Sec. I). Given the volume V and effective contact angle θ of the drops, the radius R of the spherical cap is $R = [3V/(2\pi - 3\pi\cos\theta + \pi\cos^3\theta)]^{1/3}$. We find that the length scale a follows the same scaling with θ and V as R in the $\theta \ll 1$ limit, $a \propto \theta^{-4/3}V^{1/3}$, as shown in Fig. 3(d). This length scale therefore captures the effect of geometry and size of the drops on the coalescence dynamics in the y direction.

The predicted shape of the interface in the yz plane is also in agreement with the previously established scaling for the width of the meniscus bridge. Letting $h = 0$ in Eq. (1), the half-width of the meniscus bridge becomes $r_m(t) \approx a^{1/2}\theta^2(\gamma t/\mu)^{1/2}$. For small angles, we have $\theta \approx H_0/R_0$ and $a \approx R_0^2/H_0$, which recovers the known scaling [5]. Thus, we now know the temporal scaling in both the x direction, $\theta x/vt$, and the y direction, $y/(avt)^{1/2}$. Figure 4(a) shows the temporal evolution of the 3D shape of the interface, where the surfaces formed by the markers of various shades of blue correspond to the shape of the interface at different times. Rescaling the axes with the corresponding scales collapses all of the surfaces onto a single surface, as shown in Fig. 4(b).

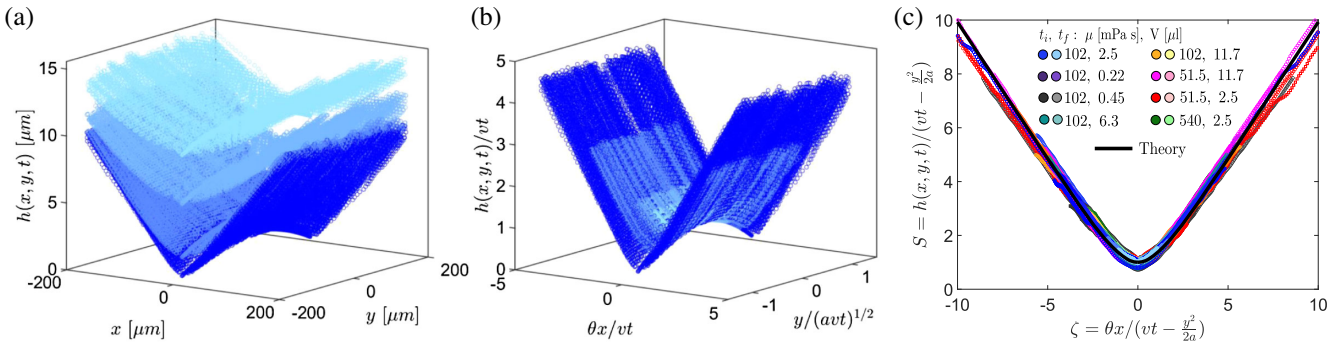

FIG. 4. The dynamic 3D interface can be mapped onto a universal curve. (a) The 3D shape of the interface at four different times during coalescence, $t = 4.8$, 7.0, 13.7, 19.6 s, with the lighter shade of blue corresponding to later times. (b) The 3D shapes of the interface collapse onto a single surface when the axes are rescaled as shown. Data are from an experiment using silicone oil drops with $\mu = 102$ mPa s, $V = 2.53$ μl, and $a = 0.01$ m. (c) Rescaling as shown in Eq. (3) gives the universal shape of the 3D interface. The experimental data are from eight experiments varying viscosity and volume of the drops as shown in the legend. The darker colored markers correspond to early times and the lighter colors markers correspond to later times during coalescence for a given experiment. For each experiment, interface profiles at four or five different times each are shown at three different y locations between 0 and 200 μm, represented by circle, square, and diamond markers. The black line is the numerical solution to Eqs. (4) and (5).

Since we know the shape of the interface along the liquid meniscus bridge, namely $h(x = 0, y, t) = vt - y^2/2a$, it is possible to further map all of the 3D interface shapes onto a universal curve using one similarity variable. Within the lubrication approximation, the evolution of the interface profile $h(x, y, t)$ is governed by

$$\frac{\partial h}{\partial t} + \frac{\gamma}{3\mu}\nabla \cdot (h^3 \nabla \nabla^2 h) = 0. \tag{2}$$

Consistent with the above results, we pose the following ansatz:

$$h(x, y, t) = \left(vt - \frac{y^2}{2a}\right) S(\zeta), \tag{3a}$$

$$\zeta = \frac{\theta x}{vt - \frac{y^2}{2a}}, \tag{3b}$$

where $vt - (y^2/2a) \geq 0$, which accounts for the time that the spreading meniscus takes to reach a specific y location from the initial coalescence point. At early times, the gradients in the y direction are much smaller than those in the x direction, i.e., $\partial/\partial y \ll \partial/\partial x$, indicating that we can neglect terms of order $[h(x = 0, y, t)/a]^2$, $(y/a)^2$ and smaller. Substituting the similarity ansatz into Eq. (2) and neglecting the small terms gives an ordinary differential equation for the self-similar shape of the 3D interface,

$$S - \zeta \frac{dS}{d\zeta} + \frac{1}{A}\frac{d}{d\zeta}\left(S^3 \frac{d^3 S}{d\zeta^3}\right) = 0, \tag{4}$$

where A is an unknown numerical prefactor from the vertical velocity of the interface $v = A(\gamma/3\mu)\theta^4$. Equation (4), which captures the dynamics of the 3D interface, is the same one that governs the self-similar height profile of the $y = 0$ plane [10]. The fourth order ordinary differential equation is subject to five boundary conditions since the value of A is also an unknown:

$$S(0) = 1, \qquad \frac{dS}{d\zeta}(0) = 0, \qquad \frac{d^3 S}{d\zeta^3}(0) = 0, \tag{5a}$$

$$\frac{dS}{d\zeta}(\infty) = 1, \qquad \frac{d^2 S}{d\zeta^2}(\infty) = 0. \tag{5b}$$

The boundary conditions enforce symmetry along the liquid meniscus bridge and a constant slope far away. We numerically solve Eqs. (4) and (5) and find a unique solution for $S(\zeta)$ and the prefactor $A \approx 0.819$.

The similarity solution $S(\zeta)$ represents the universal shape of the 3D interface near the coalescence point. The rescaled experimental data from different experiments varying the viscosity and the volume of the drop, including more than 100 different rescaled interface profiles at different times, are shown in Fig. 4(c). The numerical solution (black line) for $S(\zeta)$ is plotted on top of the experimental data and shows good agreement.

Our results provide a unified framework for understanding the coalescence of sessile and viscous drops within the thin-film approximation. Consistent with the assumptions commonly made in this problem, we provide a more general form of the similarity solution that captures the dynamics of the three-dimensional interface near the coalescence point, and that correctly reproduces and ties together the previously known scaling laws. Although interferometry constrains us to study very small effective contact angles in our experiments, we expect our results to be valid well above that range yet within the thin-film approximation that serves as the basis for our model.

Previous works have successfully used thin-film models for angles even up to 45° in some cases [10,23,24].

The comprehensive approach that we provide may be useful even beyond the thin-film limit. It will be interesting to examine the 3D self-similarity of the interface during coalescence of low-viscosity drops [8], where geometry is known to play an important role, and during asymmetric coalescence where one might expect a skewed saddle-shaped interface [10,11]. Insight into the three-dimensional shape of the interface will be valuable for the vast variety of applications involving drops and coalescence such as ink-jet printing, surface coating, and condensation [25–27].

We thank C. Kurzthaler for helpful discussions and K. Tojo for imaging the side view of the drops. We thank ExxonMobil Research and the Andlinger Center for Energy and the Environment at Princeton University for partial funding of this work. We thank the PRISM Imaging and Analysis Center at Princeton University for providing the objective lens used in the experimental setup.

*Corresponding author.
hastone@princeton.edu

[1] C. Andrieu, D. Beysens, V. Nikolayev, and Y. Pomeau, Coalescence of sessile drops, J. Fluid Mech. **453**, 427 (2002).
[2] S. J. Gokhale, S. DasGupta, J. L. Plawsky, and P. C. Wayner, Jr., Reflectivity-based evaluation of the coalescence of two condensing drops and shape evolution of the coalesced drop, Phys. Rev. E **70**, 051610 (2004).
[3] R. Narhe, D. Beysens, and V. Nikolayev, Contact line dynamics in drop coalescence and spreading, Langmuir **20**, 1213 (2004).
[4] N. Kapur and P. H. Gaskell, Morphology and dynamics of droplet coalescence on a surface, Phys. Rev. E **75**, 056315 (2007).
[5] W. D. Ristenpart, P. M. McCalla, R. V. Roy, and H. A. Stone, Coalescence of Spreading Droplets on a Wettable Substrate, Phys. Rev. Lett. **97**, 064501 (2006).
[6] R. Narhe, D. Beysens, and Y. Pomeau, Dynamic drying in the early-stage coalescence of droplets sitting on a plate, Europhys. Lett. **81**, 46002 (2008).
[7] M. W. Lee, D. K. Kang, S. S. Yoon, and A. L. Yarin, Coalescence of two drops on partially wettable substrates, Langmuir **28**, 3791 (2012).
[8] A. Eddi, K. G. Winkels, and J. H. Snoeijer, Influence of Droplet Geometry on the Coalescence of Low Viscosity Drops, Phys. Rev. Lett. **111**, 144502 (2013).
[9] Y. Sui, M. Maglio, P. D. Spelt, D. Legendre, and H. Ding, Inertial coalescence of droplets on a partially wetting substrate, Phys. Fluids **25**, 101701 (2013).
[10] J. F. Hernández-Sánchez, L. A. Lubbers, A. Eddi, and J. H. Snoeijer, Symmetric and Asymmetric Coalescence of Drops on a Substrate, Phys. Rev. Lett. **109**, 184502 (2012).
[11] H. Riegler and P. Lazar, Delayed coalescence behavior of droplets with completely miscible liquids, Langmuir **24**, 6395 (2008).
[12] S. Karpitschka and H. Riegler, Noncoalescence of Sessile Drops from Different but Miscible Liquids: Hydrodynamic Analysis of the Twin Drop Contour as a Self-Stabilizing Traveling Wave, Phys. Rev. Lett. **109**, 066103 (2012).
[13] S. Karpitschka and H. Riegler, Sharp transition between coalescence and non-coalescence of sessile drops, J. Fluid Mech. **743**, R1 (2014).
[14] R. Borcia and M. Bestehorn, Partial coalescence of sessile drops with different miscible liquids, Langmuir **29**, 4426 (2013).
[15] M. A. Bruning, M. Costalonga, S. Karpitschka, and J. H. Snoeijer, Delayed coalescence of surfactant containing sessile droplets, Phys. Rev. Fluids **3**, 073605 (2018).
[16] R. W. Hopper, Plane Stokes flow driven by capillarity on a free surface, J. Fluid Mech. **213**, 349 (1990).
[17] J. Eggers, J. R. Lister, and H. A. Stone, Coalescence of liquid drops, J. Fluid Mech. **401**, 293 (1999).
[18] R. Picknett and R. Bexon, The evaporation of sessile or pendant drops in still air, J. Colloid Interface Sci. **61**, 336 (1977).
[19] W. B. Hardy, III. The spreading of fluids on glass, London, Edinburgh, Dublin Philos. Mag. J. Sci. **38**, 49 (1919).
[20] P.-G. De Gennes, Wetting: Statics and dynamics, Rev. Mod. Phys. **57**, 827 (1985).
[21] H. P. Kavehpour, B. Ovryn, and G. H. McKinley, Microscopic and Macroscopic Structure of the Precursor Layer in Spreading Viscous Drops, Phys. Rev. Lett. **91**, 196104 (2003).
[22] See Supplemental Material at http://link.aps.org/supplemental/10.1103/PhysRevLett.129.144501 for a geometric interpretation about the interface profile in the yz plane.
[23] A. Alizadeh Pahlavan, L. Cueto-Felgueroso, G. H. McKinley, and R. Juanes, Thin Films in Partial Wetting: Internal Selection of Contact-Line Dynamics, Phys. Rev. Lett. **115**, 034502 (2015).
[24] B. Zhao, A. Alizadeh Pahlavan, L. Cueto-Felgueroso, and R. Juanes, Forced Wetting Transition and Bubble Pinch-Off in a Capillary Tube, Phys. Rev. Lett. **120**, 084501 (2018).
[25] J. Madejski, Solidification of droplets on a cold surface, Int. J. Heat Mass Transfer **19**, 1009 (1976).
[26] H. Wijshoff, The dynamics of the piezo inkjet printhead operation, Phys. Rep. **491**, 77 (2010).
[27] J. Blaschke, T. Lapp, B. Hof, and J. Vollmer, Breath Figures: Nucleation, Growth, Coalescence, and the Size Distribution of Droplets, Phys. Rev. Lett. **109**, 068701 (2012).